Use of hydrogeochemistry and environmental isotopes for evaluation of groundwater in Qingshuihe Basin, northwestern China

Xiangquan Li · Li Zhang · Xinwei Hou

Abstract Hydrogeochemistry and environmental isotope data were utilized to understand origin, geochemical evolution, hydraulic interconnection, and renewability of groundwater in Qingshuihe Basin, northwestern China. There are four types of groundwater: (1) shallow groundwater in the mountain front pluvial fans, originating from recent recharge by precipitation, (2) deep paleo-groundwater of the lower alluvial plains, which was formed long ago, (3) shallow groundwater in the lower alluvial plains, which has undergone evaporation during the recharge process, and (4) mixed groundwater (shallow and deep groundwater in the plain). The main water types are Na–HCO$_3$, which dominates type (1), and Na–SO$_4$, which dominates types (2) and (3). Geochemical evolution in the upper pluvial fans is mainly the result of CO$_2$ gas dissolution, silicates weathering and cation exchange; in the lower alluvial plains, it is related to mineral dissolution. The evaporative enrichment only produces significant salinity increases in the shallow groundwater of the lower alluvial plains. Shallow groundwater age in the upper plain is 10 years or so, showing a strong renewability. Deep groundwater ages in the lower plain are more than 200 years, showing poor renewability. In the exploitation areas, the renewability of groundwater evidently increases and the circulation period is 70–100 years.

Résumé Des données hydrogéochimiques et des données sur les isotopes de l'environnement ont été utilisées pour comprendre l'origine, l'évolution géochimique, l'interconnexion hydraulique et le renouvellement des eaux souterraines dans le basin de Qingshuihe au Nord-Ouest de la Chine. Il y a quatre types d'eaux souterraines : (1) des eaux souterraines phréatiques localisées dans les cônes de déjection au niveau des piedmonts de montagne et issues d'une recharge récente par les précipitations, (2) des eaux paléo souterraines profondes situées dans les anciennes vallées alluviales, (3) des eaux souterraines phréatiques localisées dans les basses vallées alluviales actuelles et qui ont été affectées par l'évaporation lors du processus de recharge, et (4) des eaux souterraines mélangées (eaux phréatiques et profondes, situées dans la plaine). Les principaux faciès chimiques rencontrés sont le type Na–HCO$_3$ qui domine (1) et le type Na–SO$_4$ qui domine (2) et (3). L'évolution géochimique des eaux situées dans les cônes de déjection supérieurs est principalement liée à la dissolution du CO$_2$ gazeux, à l'altération des silicates et à l'échange cationique. Dans les plaines alluviales inférieures, l'évolution géochimique est liée à la dissolution des minéraux, et le processus d'évaporation entraîne des augmentations importantes de la salinité des eaux souterraines peu profondes dans cette zone. L'âge des eaux souterraines phréatiques localisées dans la plaine supérieure est de l'ordre de 10 ans environ, indiquant un renouvellement important. L'age des eaux souterraines profondes de la plaine inférieure sont évaluées à plus de 200 ans, démontrant un taux de renouvellement faible. Dans les zones d'exploitation, le renouvellement des eaux souterraines augmente manifestement et le temps de circulation se situe entre 70 et 100 ans.

X. Li (✉) · L. Zhang · X. Hou
Institute of Hydrogeology and Environmental Geology,
Chinese Academy of Geological Sciences,
Shijiazhuang, 050061, China
e-mail: lxqlm2003@yahoo.com.cn
Fax: +86-311-8021225

Resumen Se han utilizado datos hidrogeoquímicos y de isótopos estables para entender el origen, la evolución geoquímica, la interconexión hidráulica y la renovabilidad del agua subterránea en la Cuenca Qingshuihe, al Noroeste de China. Hay cuatro tipos de agua subterránea: (1) agua superficial en los abanicos aluviales de los frentes de montaña, originadas de la recarga reciente de la precipitación, (2) paleo-aguas profundas en las llanuras aluviales bajas, que se han formado hace largo tiempo, (3) agua superficial en las llanuras aluviales bajas, que han sufrido evaporación durante el proceso de recarga, y (4) aguas subterráneas mezcla (agua superficial y profunda en la llanura). El principal tipo de agua es Na–HCO$_3$, que domina (1), y Na–SO$_4$, que domina (2) y (3). La evolución geoquímica en los abanicos aluviales superiores es fundamentalmente el resultado de la disolución de CO$_2$, de la alteración de silicatos y el intercambio de cationes; en las llanuras aluviales inferiores, están relacionadas con la disolución mineral. El enriquecimiento por evaporación solamente produce un incremento de salinidad significa-

tivo en las aguas subterráneas superficiales de las llanuras aluviales inferiores. La edad de las aguas superficiales en la llanura aluvial superior es de aproximadamente 10 años, mostrando una fuerte renovabilidad. La edad de las aguas profundas en la llanura inferior es de más de 200 años, mostrando una renovabilidad baja. En las áreas de explotación, la renovabilidad del agua subterránea evidentemente se incremente y el periodo de circulación es de 70–100 años.

Introduction

Qingshuihe Basin is located in the southern Ningxia Hui autonomous region (SNHAR), lying on the Loess Plateau of northwestern China, which is the poorest area of the country and extremely short of water resources. The area, with 6.3×10^8 m^3 total water resources and only 273 m^3/year per person, is often faced with difficulties in the supply of domestic drinking water. In normal years, about 218,000 people have no fresh water to drink, which increases to about 500,000 people in severe dry years (Chen and Ma 2000). The scarcity of water resources seriously threatens the local inhabitants' survival, and is one of main reasons for poverty in the region.

Three main characteristics of the water-related environmental conditions in SNHAR can be summarized: (1) SNHAR is in a typical continental arid climatic area, where the water circulation is not active, and surface water is very limited; (2) the complex tectonism of the region has resulted in the geomorphologic feature of mountain alternating with basin because of the presence of the "the

arc-shaped nappe tectonic belt of southern Ningxia" (Zhou 1984); the basins between the mountains are the main storage sites of groundwater and Qingshuihe Basin is one of the tectonic fault basins (Fig. 1); (3) the qualities of both surface water and shallow groundwater are very poor, and saline water is extensively distributed in the basin; shallow groundwater with total dissolve solids (TDS) concentration of more than 3 g/L occupies about 16,700 km^2, accounting for 47% of the region (NGMB 1990).

Between 1980 and 1997, more than 80 fresh groundwater extraction wells were drilled by Ningxia Geology and Mineral Bureau (NGMB) to overcome the residents' drinking water difficulties in Qingshuihe Basin (NGMB 1997). The currently exploited aquifers in the area are the shallow unconfined aquifers in the mountain front pluvial fans and the medium-deep confined aquifers in the center of the basin.

In recent years, Qingshuihe Basin has been facing increasingly serious ecological challenges due to the over-exploitation of the groundwater reservoir, including decline of groundwater quality, salt water intrusion and water-soil erosion. All of these pose a serious threat to the livelihoods of the local residents and the surrounding ecosystems. If the water resources cannot be exploited and utilized rationally, the ecological environment will deteriorate and the limited freshwater resources will become exhausted.

A series of investigations in Qingshuihe Basin has been conducted, beginning in the early 1980s, to improve understanding of the hydrogeologic framework and hydrologic conditions in the aquifer system and to calculate the groundwater resource volume by developing groundwater-flow models (NGMB 1984, 1990, 1997). However, groundwater management in Qingshuihe Basin

Fig. 1 Hydrogeological map of the southern Ningxia Hui autonomous region (SNHAR) in China
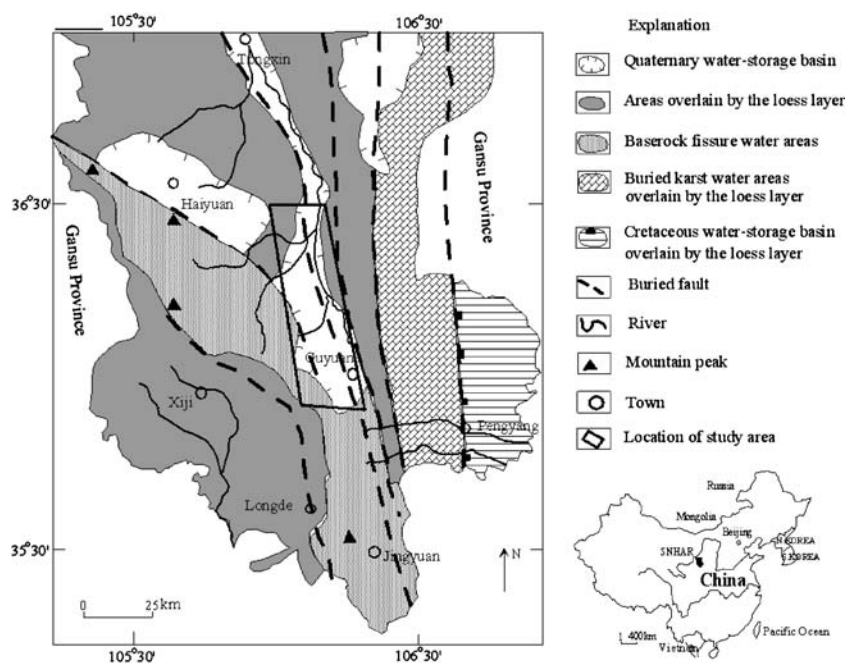
is often faced with the difficult task of explaining the origin, evolution and renewability of groundwater in aquifers prone to over-exploitation. The reasons are related to insufficient hydrological, geophysical and hydrochemical data, and an often complex aquifer system with horizontal and vertical groundwater flow components.

The purpose of this study has been, thus, to use environmental isotope techniques and a geochemical model to make a new assessment of the availability of groundwater resources in the aquifer on the basis of a better understanding of hydrogeological features. This includes explanation of groundwater origin, identification of hydraulic interconnection between aquifer systems, tracing of the geochemical evolution of groundwater, and estimation of groundwater renewability, as well as focusing on the impact of intensive groundwater pumping from this aquifer system. A similar approach was used to interpret the geochemical evolution in regional aquifers by Hendry and Schwartz (1990), Weaver and Bahr (1991), Gerla (1992), Sracek and Hirata (2002), Mahlknecht and Schneider (2004) and others.

Study area

General description
The Qingshuihe Basin is an intermountain sedimentary basin extending from south to north which covers about 766 km^2. The basin is partly surrounded by mountain ranges, which include Liupanshan Mountains to the south and west; and the Loess Hills to the east (Fig. 2). The terrain of the basin gradually becomes lower from south to north, with the lowest elevations of 1,400 m above sea level (asl) and summits of 1,850 m (Zhou 1984).

The climate of the whole Qingshuihe Basin is semi-arid, although parts of the surrounding mountainous areas are humid. Mean annual precipitation (monitored from 1973 to 2001 at five meteorological stations) was 600 mm in Liupanshan Mountains piedmont, and 300 mm in the northern plain. The high rainfall season is from July to September, with 75 to 111 mm/month. The range of precipitation during the dry season from October to June is from 2.5 to 42.1 mm/month, with December being the driest month. The mean annual temperature and the mean summer temperature are 6.3 and 19°C, respectively (Ningxia Meteorological Bureau of China 1995).

The main stream, the Qingshuihe River, extends the entire length of the eastern side of the basin, with headwaters in Liupanshan Mountains. The river leaves the basin at the northern border of the study area, where it eventually converges with Huanghe River. The water quality of Qingshuihe River deteriorates from upstream (at Guyuan station, with TDS <1 g/L) to downstream (at the border of the study area, with TDS 6 g/L). Several tributaries, including Dongzhihe River, Zhonghe River and Xianmahe River, contribute substantial flow to Qingshuihe River, and, potentially, can contribute substantial quantities of recharge to the underlying aquifer system.
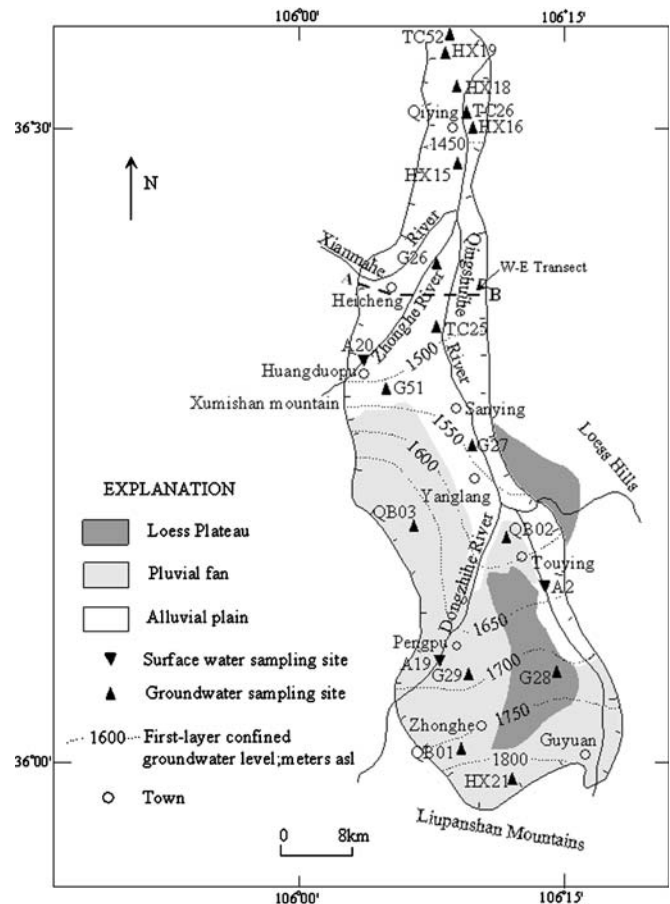

Fig. 2 Geomorphologic map of Qingshuihe Basin; cross-section AB is shown in Fig. 3

Geologic and hydrogeologic settings
The Qingshuihe Basin was formed during the Himalayan movement period in the Tertiary Period. A deep compressed fracture passes by the western and southern boundaries of the study area, and deep tensional fractures underlie the eastern boundary. The base rocks are thick Tertiary and Lower Cretaceous formations; the former consist of red sandy mudstone interbedded with gypsum beds, while the latter is blue-gray mudstone and marl with high content of salt (Fig. 3).

From the hydrogeological point of view, the upper part of the aquifer consists of alluvial to lacustrine sandy to silty sediments formed during the early, middle and late Pleistocene of the Quaternary Period. There are three water-bearing formations according to the burial conditions: shallow unconfined aquifer, deep first-layer confined aquifer and deep second-layer confined aquifer.

The total groundwater recharge volume in the study area, according to a water balance approach, is 44 million m^3/year (NGMB 1984). Figure 2 presents the present-day groundwater level configuration in the first-layer confined aquifer (NGMB 2000). The groundwater levels indicate that groundwater movement in the first-layer confined aquifer through the central part of the basin has been primarily oriented south to north. Near the basin margins, groundwater flow in this aquifer has been oriented toward

Fig. 3 Geological cross-section of Qingshuihe Basin through Heicheng
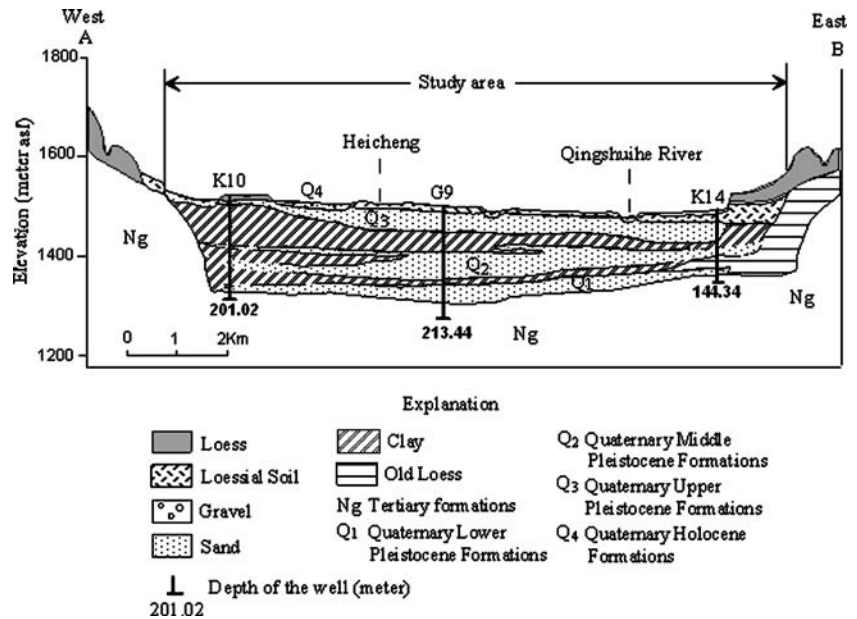
the central part of the basin. The groundwater flows in the other aquifers have the same directions as the first-layer confined aquifer. Groundwater discharge to streams and springs from the unconfined aquifer is thought to be reducing at the present time, due to the relatively deep groundwater level in most of the basin and the decreasing number of springs. The small depressions in the water table have been made by the intensive groundwater extraction in some places.

Methodology

The sampling campaign was undertaken in the study area during September 2000. Sixteen sets of samples were taken from agricultural and domestic water production wells for hydrochemical and environmental isotopic analysis. Wells draw from both shallow and deep groundwater in the basin. There are three sets of surface water samples from the rivers of the basin. The sampling sites are shown in Fig. 2.

The samples destined for anion and cation analysis were filtered (0.45 μm) and stored with tri-distillate water, in new pre-rinsed HDPE bottles (Nalgene) at a constant temperature of 4°C. Additionally, cation samples were acidified to a pH<2 by ultrapure nitric acid. The cations and anions were determined by the Laboratory of Hydrogeology and Environmental Geology Institute, Chinese Academy of Geological Sciences (CAGS), with inductive-coupled plasma mass spectrometry (ICP-MS) and ion chromatography, respectively.

Analyses of the stable isotopes were carried out using a mass spectrometer for stable isotopes at the Laboratory of Hydrogeology and Environmental Geology Institute, CAGS. The D/H (deuterium/hydrogen) ratio was measured by the method of Bigeleisen et al. (1952), and the $^{18}O/^{16}O$ ratio was measured by a CO_2 equilibrium method

(Epstein and Mayeda 1953). The δ-values are defined conventionally as

$$\delta(^0\!/_{00}) = \left(R_{\text{sample}} - R_{\text{SMOW}}\right)/R_{\text{SMOW}} \times 1000$$

where R_{sample} is the mass ratio of the stable isotope (D/H or $^{18}O/^{16}O$) and R_{SMOW} is the value for the Standard Mean Ocean Water. The precision of measurements is better than ±0.1‰ for $\delta^{18}O$ and ±1‰ for δD. Tritium (after electrolysis) was measured with a liquid scintillation counter (Quantulus1220). The ^{3}H content is reported in tritium units (TU). The precision of measurements is better than ±0.2 TU.

Results

Hydrochemical results

The chemical constituents of the water samples are shown in Table 1. The values of pH for the shallow groundwater in the mountain front pluvial fans, the shallow groundwater in the lower alluvial plains, the deep groundwater in the mountain front pluvial fans, and the deep groundwater in the lower alluvial plains ranges from 7.7~8.8 (average of 8.1), 7.6~8.2 (average of 8), 7.5~7.9 (average of 7.6), and 7.6~8.3 (average of 8), respectively. The pH values of the water samples from unconfined aquifers are commonly higher than those of the water samples from confined aquifers. It is necessary to state that the deep groundwater in the mountain front pluvial fans is an intermediate type between the shallow groundwater in the mountain front pluvial fans and the deep groundwater in the lower alluvial plains. This type of groundwater has many characteristics of the mixed groundwater.

The average values for TDS in the shallow groundwater in the mountain front pluvial fans, the shallow

Table 1 Hydrochemical data for groundwater and surface water

Sample code	Location	Source	Hydrochemical zone	Temp. (°C)	pH	K+ (mg/L)	Na+ (mg/L)	Ca2+ (mg/L)	Mg2+ (mg/L)	Cl- (mg/L)	SO4 2- (mg/L)	HCO3- (mg/L)	CO3 2- (mg/L)	NO3- (mg/L)	TDS (mg/L)
G27	Sanying	Unconfined aquifer	Middle Alluvial Plain	20	7.7	3.58	336.49	47.08	57.57	54.82	504.91	555.23	0.0	23.13	1,582.8
G28	Touying	Unconfined aquifer	Mountain Front Pluvial Fan	23	8.8	1.92	227.06	7.85	15.94	19.22	56.41	534.56	14.52	16.36	893.9
QB01	Zhonghe	Unconfined aquifer	Mountain front pluvial fan	17	8.0	2.07	171.27	22.36	23.31	10.68	47.01	517.43	0.0	26.22	820.4
QB03	Yanglang	Unconfined aquifer	Mountain front pluvial fan	16	8.0	1.67	147.62	19.62	32.12	17.8	84.62	460.73	0.0	15.46	779.6
TC25	Sanying	Unconfined aquifer	Lower alluvial plain	22	7.6	3.75	204.28	105.09	89	156.39	558.72	325.07	0.0	0.0	1,442.9
TC26	Qiying	Unconfined aquifer	Lower alluvial plain	20	8.2	6	703.07	160.76	143.78	480.7	1,400.68	385.41	0.0	28.57	3,308.9
TC52	Qiying	Unconfined aquifer	Lower alluvial plain	21	8.2	10.5	1,444	485.97	275.27	1,311.76	3,333.42	289.83	0.0	11	7,161.7
HX21	Zhonghe	Confined aquifer	Mountain front pluvial fan	12	7.9	2.5	68.02	91.48	40.93	21.79	242.67	352.32	0.0	4.43	824.1
G29	Pengpu	Confined aquifer	Mountain front pluvial fan	16	7.5	1.89	75.28	63.55	42.35	12.81	125.05	413.47	0.0	13.76	748.2
QB02	Touying	Confined aquifer	Mountain front pluvial fan	13	7.6	2.66	166.06	80.42	75.42	135.26	371.39	330.78	0.0	7.82	1,169.8
G51	Huangduopu	Confined aquifer	Middle alluvial plain	15	7.5	3.51	166.8	131.42	142.03	201.47	663.34	315.42	0.0	36.85	1,660.8
G26	Heicheng	Confined aquifer	Lower alluvial plain	14	7.6	4.77	672.16	121.61	90.4	498.33	1,069.52	336.68	0.0	10.89	2,804.4
HX15	Qiying	Confined aquifer	Lower alluvial plain	12	8.1	6	482.54	163.42	119.01	465.32	925.98	328.96	0.0	10.26	2,501.4
HX16	Qiying	Confined aquifer	Lower alluvial plain	14	8.2	5.5	557.59	122.57	99.08	403.79	1,015.38	340.64	0.0	10.38	2,554.9
HX18	Qiying	Confined aquifer	Lower alluvial plain	15	8.2	6	965.07	150.99	123.31	682.60	1,594.39	346.48	0.0	22.66	3,891.5
HX19	Qiying	Confined aquifer	Lower alluvial plain	13	7.8	8.5	700.13	254.91	234.78	826.81	1,602.9	251.1	0.0	28.4	3,907.5
A2	Qingshuihe River	Surface water		25	7.7	24.25	150.93	76.88	49.52	101.87	297.49	386.68	0.0	24.52	1,112.1
A19	Dongzhihe River	Surface water		25	8.0	6	744	175.35	84.46	418.35	1,484.19	323.39	3	2	3,240.7
A20	Zhonghe River	Surface water		25	8.3	8.5	1,416	470.94	130.04	925.32	3,047.63	109.83	0.0	7.5	6,115.7

340

groundwater in the lower alluvial plains, the deep
groundwater in the mountain front pluvial fans, and the
deep groundwater in the lower alluvial plains are 908,
3993.65, 1,062.62 and 3,023.12 mg/L, respectively. The
hydrogeochemical data show that fresh groundwater zones
in the basin are mainly in the mountain front pluvial fans,
and the saline water zones in the lower alluvial plains. The
average value for TDS in the shallow groundwater in the
lower alluvial plains is the highest among the above four
kinds of groundwater. The TC52 water sample, with high
TDS of 7,183.04 mg/L, would be affected by the mixing
of the groundwater with surface water with high TDS. The
spatial distribution of TDS in the confined groundwater is
shown in Fig. 4. The value of TDS becomes higher along
the groundwater flow from south to north.

The waters are categorized according to their content of
major cations and anions by using a Piper diagram
(Fig. 5). In the study area, the most common water types
among the groundwater samples analyzed are Na–SO$_4$ and
Na–HCO$_3$, followed by mixed-cation-HCO$_3$ and mixed-
cation-SO$_4$. Different water types tend to group in distinct
water-bearing formations and zones of the basin. The Na–
HCO$_3$ type generally dominates the shallow, unconfined
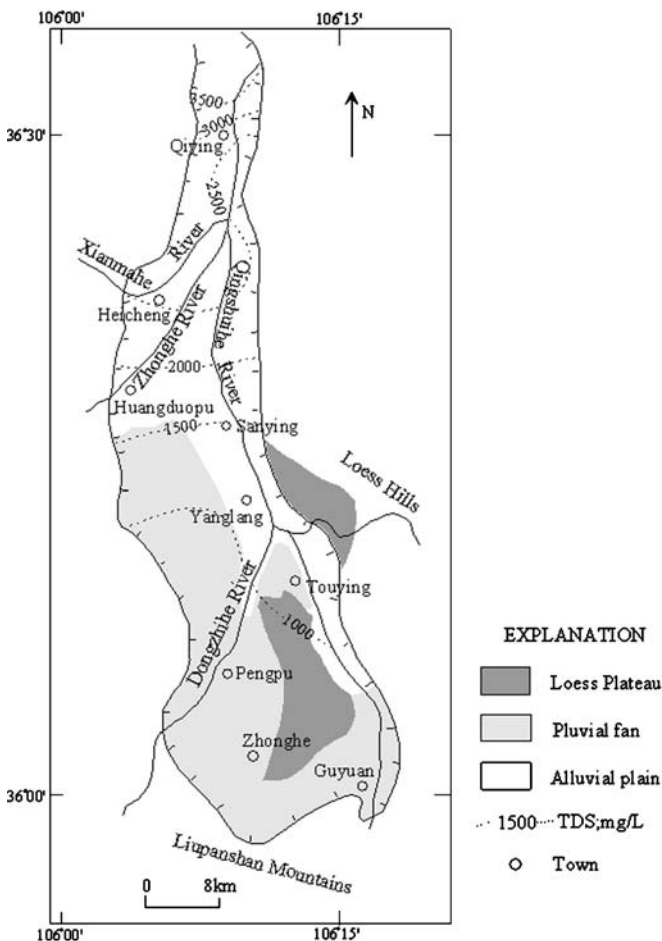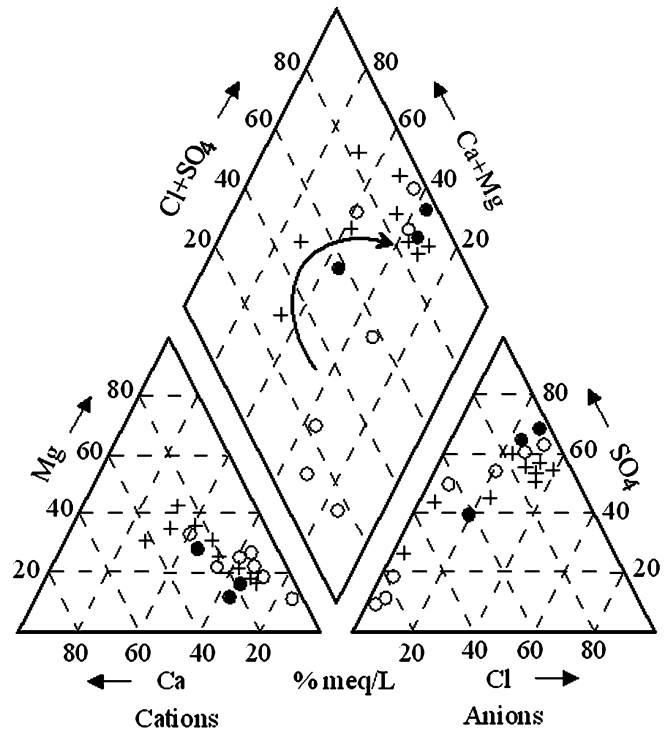zones of the mountains front pluvial fans, whereas the

Fig. 5 Piper diagram of groundwater and surface water samples

Fig. 4 Spatial distribution of total dissolved solids (TDS) in the
confined groundwater (in mg/L)

Na–SO$_4$ dominates the shallow, unconfined and deep,
confined zones of the lower alluvial plain. The mixed-
cation-HCO$_3$ type dominates the deep confined zones of
the mountains front pluvial fans. The mixed-cation-SO$_4$
samples are relatively common near the deep confined
zones of the transitional areas between the mountains front
pluvial fans and the alluvial plains. There is no Cl-type of
groundwater in the study area.

The most striking feature is the evolution from Na–
HCO$_3$ water in the upper pluvial fans towards Na–SO$_4$
water with increased SO$_4^{2-}$ and Cl$^-$ concentrations in the
lower alluvial plains. For shallow groundwater, concen-
trations of Na$^+$ in the southern pluvial fans are less than
100 mg/L but they reach more than 1,400 mg/L in the
northern alluvial margin of the basin. Concentrations of
SO$_4^{2-}$ also increase from values less than 200 mg/L to
values of more than 3,300 mg/L. Concentrations of Cl in
the upper pluvial fans are less than 20 mg/L but later reach
1,300 mg/L further north. The nitrate concentration ranges
from 4.43 mg/L to 36.85 mg/L. All water samples have
less NO$_3^-$ than the maximum amount of 45 mg/L
permitted by the US Environmental Protection Agency
(US EPA 2003).

Isotopic results

The $\delta^{18}O$, δ^2H and ^3H data of the groundwater samples range from $-11.5 \sim -8.2‰$, $-83.8 \sim -53.63‰$, and $3.48\sim23.09$ TU, respectively. The corresponding average values are $-9.98‰$, $-67.79‰$ and 13.56 TU (Table 2). The mean isotopic concentration of rainwater from which the groundwater was derived suggests that the mean ^{18}O of rainfall events resulting in recharge is about $-11.5‰$. The value corresponds to the most isotopically depleted groundwater samples, and represents therefore the largest rainfall events in the region and/or groundwater infiltrated at higher elevations. The most ^{18}O enriched groundwater ($-8.2‰$) represents lower elevations and/or short rainfall events.

The isotopic data of the groundwater was divided into four homogeneous types according to the distribution of data points in Fig. 6. Type A includes G28 and G27, which are in the top right of Fig. 6. δ^2H, $\delta^{18}O$ and ^3H values of type A are within the ranges of $-54.92 \sim -53.63‰$, $-9.23 \sim -9.09‰$, and $22.28\sim23.09$ TU, respectively. Type B including HX15, HX16, HX18 and HX19 is distributed in the bottom left of Fig. 6, and the stable isotope values are the lowest in the four types. δ^2H, $\delta^{18}O$ and ^3H values of type B are within the ranges of $-80.4\sim-79.6‰$, $-11.5\sim-10.8‰$ and 3.48–5.43 TU, respectively. Type C including TC25, TC26 and TC52 is on the right of the diagram. δ^2H, $\delta^{18}O$ and ^3H values of type C are within the ranges of $-63.02\sim-60‰$, $-8.6\sim-8.2‰$ and 15.29–20.2 TU, respectively. The final group is type D whose data points distribute in the linear form between the above type A and type B.

The t-test algorithm has been used to verify the classification. The t-test assesses whether the means of two groups are statistically different from each other. The method was explained in detail by Lowry (1999). Table 3 shows T-values of the different groundwater types. T_{cal} and $T_{std}(\alpha=0.05)$ indicate the T-value of calculation and T-value of standard table, respectively. D_f indicates the
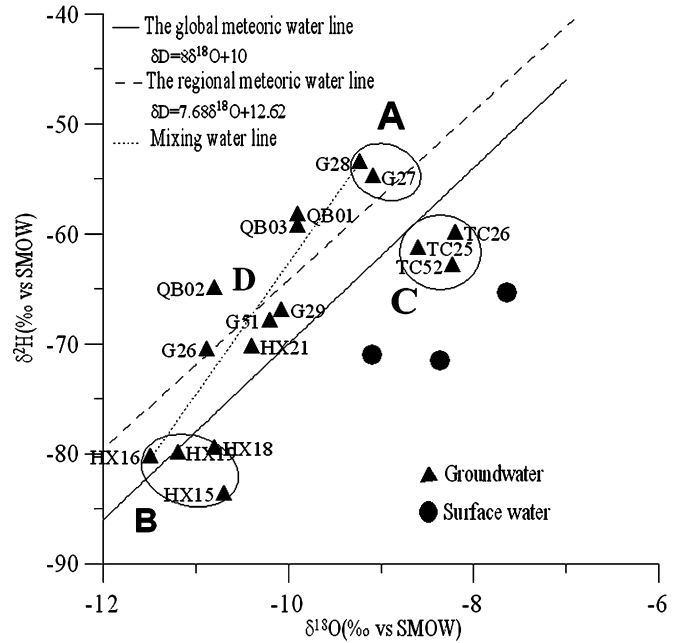

Fig. 6 Relationship between δ^2H and $\delta^{18}O$ in groundwater of Qingshuihe Basin

degree of freedom. $T_{cal}>T_{std}$ means that the T-value is large enough to be significant.

Type A represents the shallow groundwater in the mountains front pluvial fans. The isotopic data points of type A fit nicely with the regional meteoric water line (RMWL), evidently implying that groundwater is recharged by the recent atmospheric precipitation. Type B represents the deep groundwater of the lower alluvial plains. The lowest ^3H concentrations imply that this type of groundwater would be formed a long time ago, belonging to paleo-groundwater, and has little connection to the recent atmospheric precipitation. Type C represents the shallow groundwater in the lower alluvial plains; this

Table 2 Isotopic data for groundwater and surface water

Sample code	Source	Hydrochemical zone	Groundwater type	δD (‰ vs. SMOW)	δ¹⁸O (‰ vs. SMOW)	³H (TU)
G27	Unconfined aquifer	Middle alluvial plain	A	−54.92	−9.09	22.28
G28	Unconfined aquifer	Mountain front pluvial fan	A	−53.63	−9.23	23.09
QB01	Unconfined aquifer	Mountain front pluvial fan	D	−59.4	−9.9	21.5
QB03	Unconfined aquifer	Mountain front pluvial fan	D	−58.4	−9.9	19.2
TC25	Unconfined aquifer	Lower alluvial plain	C	−61.43	−8.6	19.74
TC26	Unconfined aquifer	Lower alluvial plain	C	−60	−8.2	15.29
TC52	Unconfined aquifer	Lower alluvial plain	C	−63.02	−8.23	20.2
HX21	Confined aquifer	Mountain front pluvial fan	D	−70.4	−10.4	11.84
G29	Confined aquifer	Mountain front pluvial fan	D	−67.06	−10.08	13.81
QB02	Confined aquifer	Mountain front pluvial fan	D	−65.1	−10.8	6.5
G51	Confined aquifer	Middle alluvial plain	D	−68	−10.2	12.88
G26	Confined aquifer	Lower alluvial plain	D	−70.61	−10.89	10.72
HX15	Confined aquifer	Lower alluvial plain	B	−83.8	−10.7	6.69
HX16	Confined aquifer	Lower alluvial plain	B	−80.4	−11.5	5.43
HX18	Confined aquifer	Lower alluvial plain	B	−79.6	−10.8	3.48
HX19	Confined aquifer	Lower alluvial plain	B	−80	−11.2	4.36
A2	Surface water			−71.54	−8.366	16.21
A19	Surface water			−71	−9.1	13.83
A20	Surface water			−65.34	−7.645	16.51

342

Table 3 *T*-values of the different groundwater types

Groups	Isotope	D_f	T_{cal}	T_{std} ($\alpha=0.05$)	Conclusion
Type A and type C	$\delta D(‰)$	3	6.63	3.18	Significant
	$\delta^{18}O(‰)$	3	5.57	3.18	Significant
Type A and type D	$\delta D(‰)$	7	5.71	2.37	Significant
	$\delta^{18}O(‰)$	7	6.82	2.37	Significant
Type D and type B	$\delta D(‰)$	9	7.31	2.26	Significant
	$\delta^{18}O(‰)$	9	3.08	2.26	Significant

type of groundwater has undergone evaporation during the recharging process, as indicated by the evident displacement from RMWL. Type D shows the isotopic characteristics of mixed groundwater. It also indicates that there is certain hydrologic connection between shallow groundwater and deep groundwater in the plain, and they can mix with each other.

The $\delta^{18}O$, δ^2H and ^3H values of the surface water samples range are $-9.1 \sim -7.64‰$, $-71.54 \sim -65.34‰$ and $13.83 \sim 16.51$ TU, respectively. Apparently, the surface waters have undergone evaporation because the data points follow a trend to the right of the RMWL with a slope between 2.5 and 3.5.

Discussion

Mechanism of hydrogeochemical evolution

To reveal the mechanism of hydrogeochemical evolution, the relationship between TDS and Na/Cl ratios was plotted (Fig. 7). The plot shows two patterns of data points, indicating that these two kinds of groundwater samples have different mechanisms of hydrogeochemical evolution. Na/Cl is the ratio of Na+ and Cl– concentrations which is often used to identify groundwater origin and the sources of the groundwater chemical constituents.
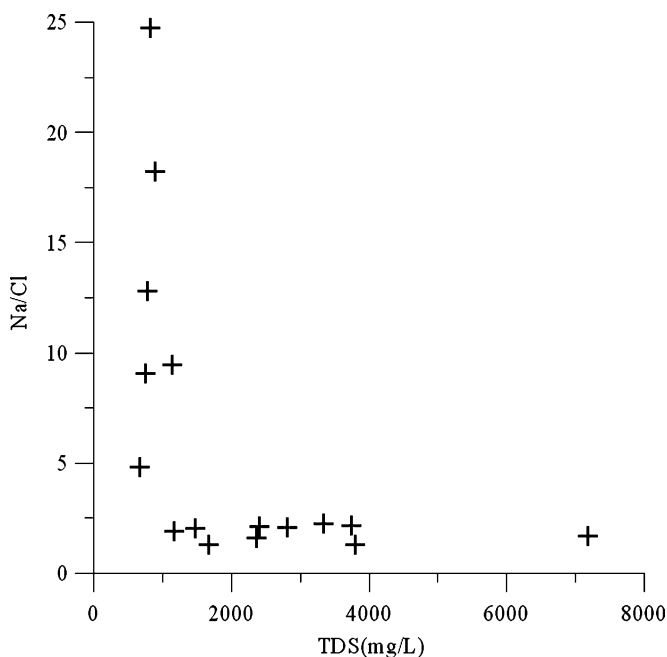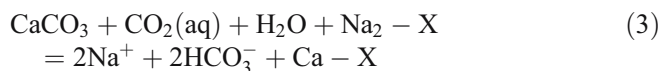
The first group of data points actually represents the fresh groundwaters in the upper pluvial fans. The most common water type is Na–HCO_3. The values of TDS are mostly less than 1 mg/L. The Na/Cl ratio ranges from 4.8 to 24.7. In this area, the groundwater is mainly recharged by the recent atmospheric precipitation and its circulation is active. This being so, the most likely mechanism that can increase concentrations of Na+ and HCO_3^- is alteration of silicates like albite in the reaction:

$$NaAlSi_3O_8 + CO_2(aq) + 11/2H_2O \rightarrow Na^+ + 1/2Al_2Si_2O_5(OH)_4 + 2H_4SiO_4 + HCO_3^- \quad (1)$$
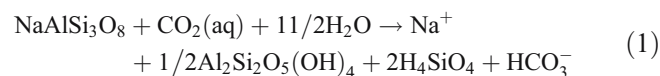
This reaction increases concentrations of Na+ and HCO_3^-, consumes $CO_2(aq)$, and thus decreases the partial pressure of carbon dioxide (P_{CO_2}) and increases pH. However, there is no net increase of total inorganic carbon concentration. Alteration of albite is an incongruent reaction with the resulting formation of kaolinite, and the original ratio of Na/Si, which is 1:1 in albite, changes to 1:2 in groundwater. Furthermore, this reaction is kinetically constrained. The dissolution of silicates probably plays a significant role in the recharge zone, in soils with low carbonate content, but contributes only very low mineralization to groundwater. Another possible reaction is cation exchange, which is

$$Ca^{2+} + Na_2 - X = 2Na^+ + Ca - X \quad (2)$$

where X denotes cation-exchange sites. In the cation exchange processes, the clay particles of the aquifer exchange calcium against sodium to elevate sodium concentrations. The sources of calcium are the dissolution of calcite and dolomite minerals in the aquifers. The overall reaction is

$$CaCO_3 + CO_2(aq) + H_2O + Na_2 - X = 2Na^+ + 2HCO_3^- + Ca - X \quad (3)$$

This reaction increases sodium and bicarbonate concentrations and decreases calcium concentrations.

The second group of data points actually represents the salty groundwater in the lower alluvial plains. The groundwater is mainly of the Na–SO_4 type with TDS of 1–3.8 mg/L. The Na/Cl ratio ranges between 1.3 and 2.2, implying that the geochemical evolution of groundwater is related to the mineral dissolution. In the light of the correlation analysis of the major ions vs. TDS (Fig. 8), the value of TDS relates well to SO_4^{2-}, Na+ and CL^- (coefficient of determination, $r^2=0.99$, 0.95, and 0.97, respectively). A possible reaction is input of Na+, SO_4^{2-} and Cl^- by dissolution of halite (NaCl) and mirabilite ($Na_2SO_4 \times 10H_2O$) deposited in the Tertiary Formation. Dissolution of both minerals is congruent and there a ratio

**Fig. 7** Relationship between Na/Cl ratio and TDS

Fig. 8 a−h Diagrams of variations between TDS and major ions in the groundwater
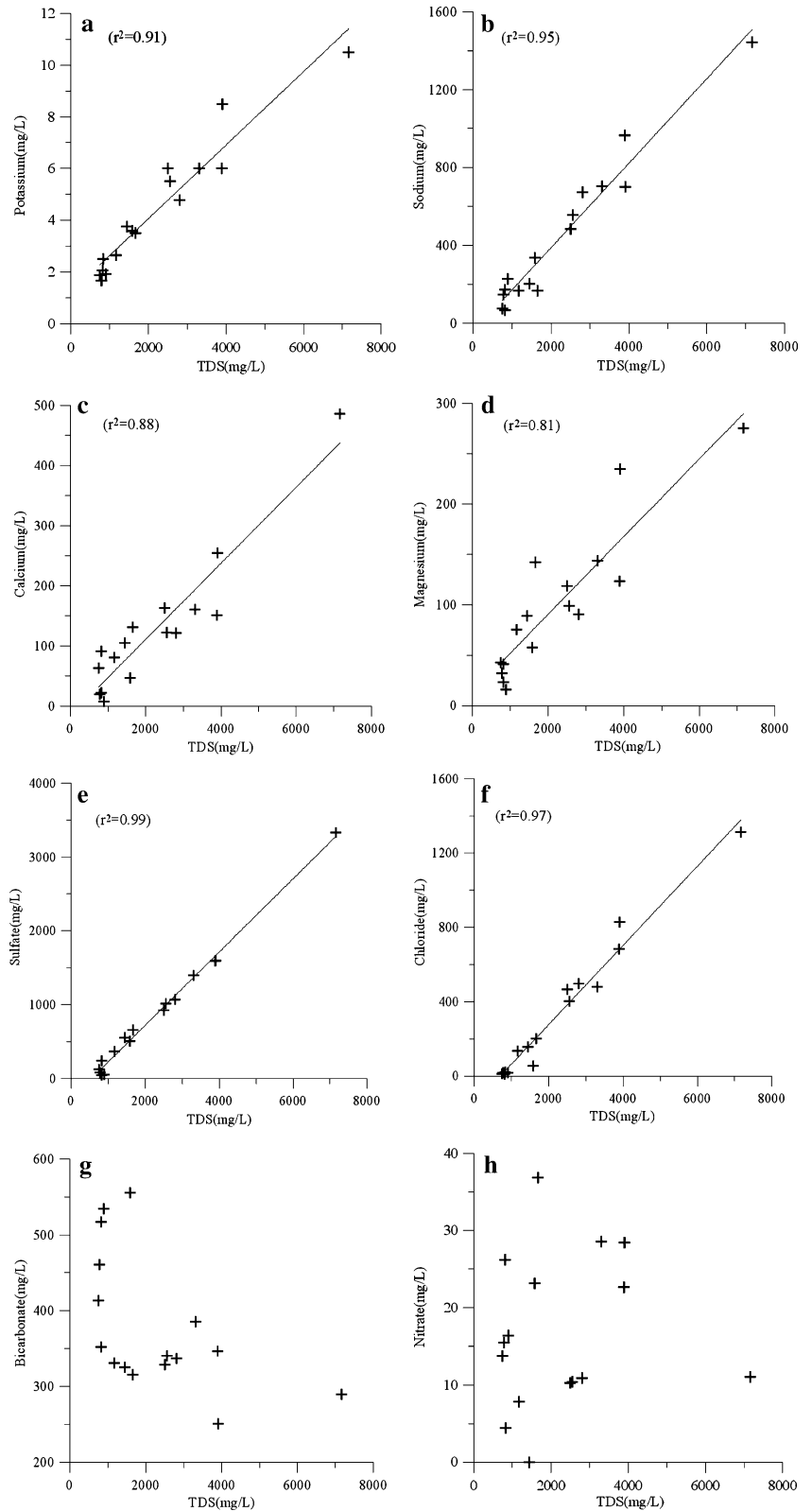
1:1 between Na and Cl in the case of halite, and a ratio 2:1 between Na^+ and SO_4^{2-} in the case of mirabilite. Both minerals are very soluble and their dissolution increases Na^+, Cl^- and SO_4^{2-} concentrations.

Another possible source of SO_4^{2-} would be dissolution of gypsum. Both Ca^{2+} and SO_4^{2-} can contribute to groundwater in the reaction. In the plots of Fig. 8, Ca^{2+} data also show a strong correlation (r^2=0.88) with TDS,

Fig. 9 Spatial distribution of the saturation indices (SI) of the major minerals **a** calcite, **b** dolomite and **c** gypsum
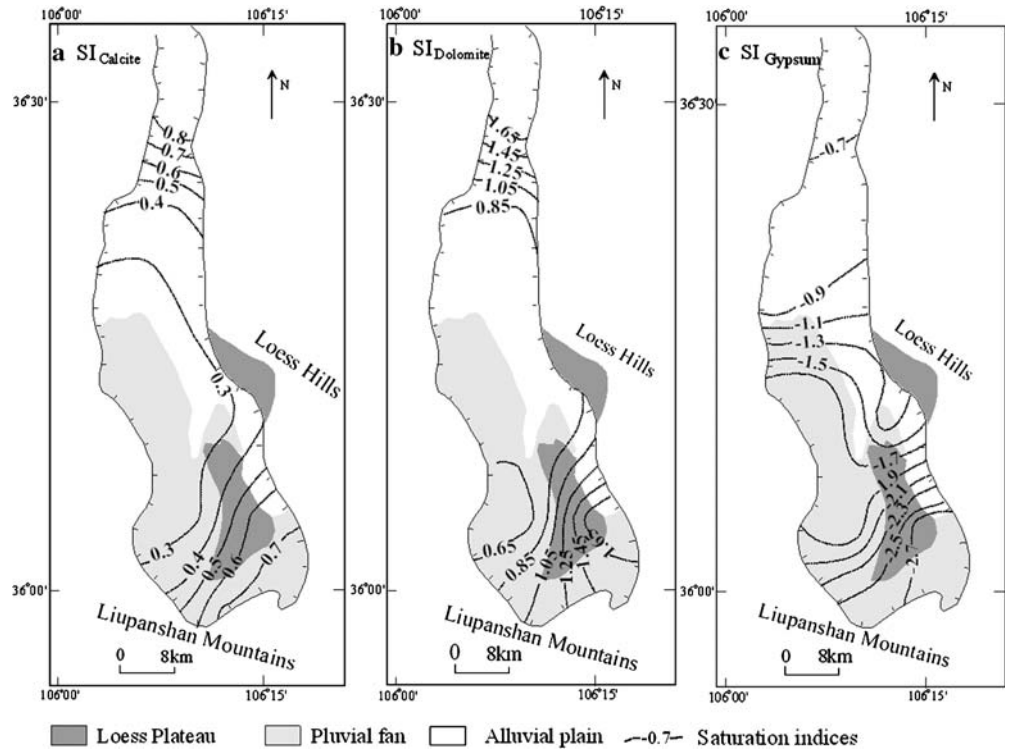
indicating that Ca^{2+} and SO_4^{2-} are derived from the same source of gypsum.

Saturation indices for selected minerals calculated by the program PHREEQC (Parkhurst 1995) are presented in Fig. 9. Saturation indices of the groundwater samples from the basin aquifers reveal that water is generally undersaturated with respect to gypsum and halite; and supersaturated with calcite and dolomite. This suggests that the groundwater can dissolve a lot of minerals such as gypsum and halite because of the slow circulation of groundwater in the process of the groundwater flow from south to north, and leads to the high value of TDS of the groundwater downgradient.

The evaporation effect generally makes a significant impact on the evolution of groundwater in the semi-arid and arid regions. The isotopic evidence can interpret the geochemical mechanism of groundwater caused by the evaporation effects. If salinity is due to the enrichment of salts by evaporation, then the $^{18}O-^2H$ signature would have a low slope reflecting kinetic fractionation. In addition, a plot of chloride content against either isotope ^{18}O or ^2H will be positively correlated, as increased evaporation would result in isotopic enrichment as well as an increased chloride concentration. If salinity is due to the leaching of evaporitic salts by rapid percolation through preferential pathways, then the groundwater should retain an $^{18}O-^2H$ relationship similar to that of regional rainfall. As the leaching process does not affect the isotopic composition of water, there would be no correlation between isotope content and chloride concentration (Payne 1988).

As shown in Figs. 10 and 11, only a few data points that represent the shallow groundwater present a positive correlation between ^{18}O and chloride or TDS, and $\delta^{18}O$ is approximately in inverse proportion to chloride and TDS for the majority of data points. The plots indicate that the evaporative enrichment only produces significant salinity increases of the shallow groundwater in the lower alluvial
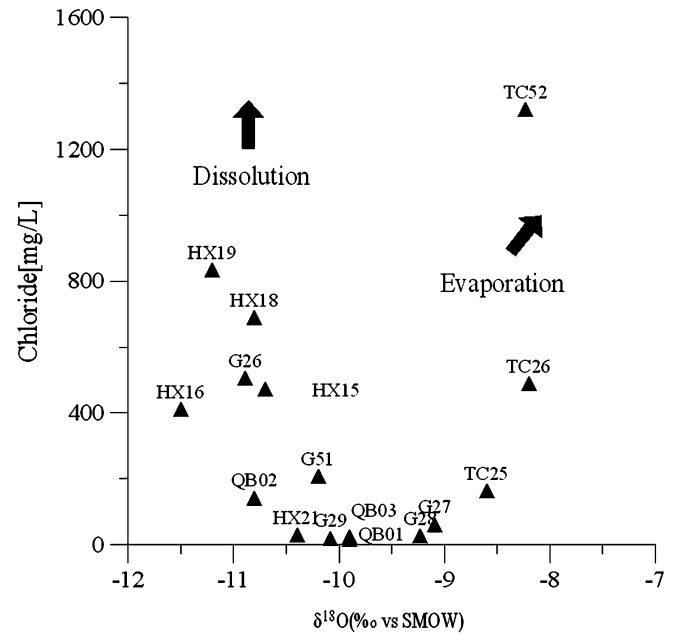

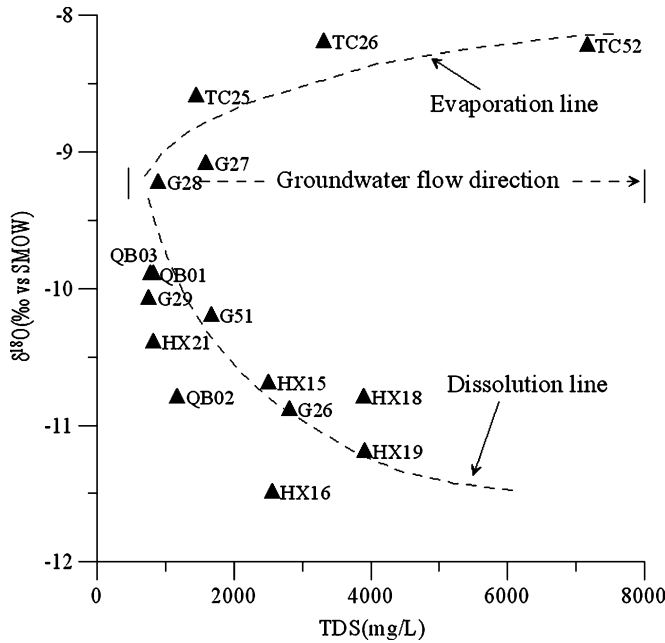
Fig. 10 Relationship between $\delta^{18}O$ and Cl^-

Fig. 11 Relationship between TDS and $\delta^{18}O$

plains and the majority of processes are dissolution oriented, which is in agreement with the corresponding saturation indices. The salinization development trend is consistent with the direction of groundwater flow, indicating that groundwater dissolves a large amount of highly soluble and less soluble salts in the course of flow northwards with a result of more serious salinization.

Mixing relationship between modern groundwater and paleo-groundwater

To further clarify the mixing relationship between shallow modern groundwater and deep paleo-groundwater under the present exploitation conditions, the ratio for the mixture has been calculated by using the binary mixing model (BM) based on the conservation of mass, both for stable isotope and for groundwater flow—Eq. (4) and Eq. (5), respectively—as follows:

$$\delta_m Q_m = \delta_1 Q_1 + \delta_2 Q_2 \qquad (4)$$

$$Q_m = Q_1 + Q_2 \qquad (5)$$

where δ_m is the concentration of stable isotope in the mixture, δ_1 is the concentration of stable isotope in the end member of shallow modern groundwater, δ_2 is the concentration of stable isotope in the end member of deep paleo-groundwater, Q_m is the volume of the mixture, Q_1 is the volume of the end member of shallow modern groundwater, Q_2 is the volume of the end member of deep paleo-groundwater. The groundwater in sampling site G28 has been selected as the end member of shallow modern groundwater and the groundwater in sampling site HX16 has been selected as the end member of deep paleo-groundwater. The ratio of the mixture between the shallow modern groundwater and the deep paleo-groundwater is defined as

$$Q1/Q2 = (\delta_m - \delta_2)/(\delta_1 - \delta_m) \qquad (6)$$

The δD and $\delta^{18}O$ values of the water sample are substituted into Eq. 6 respectively, then the average value of two ratios is obtained. The calculation results are shown in Table 4.

From the results, it can be seen that the ratio of the mixture between shallow modern groundwater and deep paleo-groundwater in the mountain front pluvial fans (QB01, QB03) is 7.5:2.5. The bigger percentage of modern groundwater shows that the recharge conditions in the hydrogeological unit are good and water circulation is strong. The mixed ratio of shallow modern groundwater and deep paleo-groundwater in the lower plain (G26) is 3.2:6.8. The lower percentage of modern groundwater indicates that there are poor recharge conditions and weak water circulation. So, generally speaking, along the groundwater flow direction, the water circulation is getting weaker from the upper reaches to the lower reaches. However, some sites in the upper plain (Pengbao exploitation area and Huangduobao exploitation area) do not follow the changing trend; the mixed ratio of shallow modern groundwater and deep paleo-groundwater is 5.2:4.7~6.6:3.4. The percentage of modern groundwater is relatively high in G29 and G51, amounting to 52−66%. These sampling sites are distributed in the area which has fresh groundwater or slightly saline groundwater (Pengbao exploitation area and Huangduobao exploitation area). Due to the over-exploitation of groundwater, there are cones of depression in the water table at a local scale. Thus, the hydrodynamic conditions for the mixing of shallow groundwater and deep groundwater increase, with a result

Table 4 Mixed proportion of groundwater

Mixed groundwater Sample code	Source	Hydrochemical zone	Modern water percentage %	Ancient water percentage %	Groundwater flow direction
QB01	Unconfined aquifer	Mountain front pluvial fan	75	25	The general direction of
QB03	Unconfined aquifer	Mountain front pluvial fan	77	23	the groundwater flow in
HX21	Confined aquifer	Mountain front pluvial fan	43.5	56.5	Qingshuihe Basin is just
G29	Confined aquifer	Mountain front pluvial fan	66	34	from QB1 point to G26
QB02	Confined aquifer	Mountain front pluvial fan	44	56	point
G51	Confined aquifer	Middle alluvial plain	52.5	47.5	
G26	Confined aquifer	Lower alluvial plain	32	68	

346

that shallow groundwater recharges deep groundwater by way of the leakage.

Flow pattern of groundwater recharge

Through the spatial distribution analysis of the isotopic data, it can been seen from the $\delta^{18}O$ and ^3H isopleths shown as in Fig. 12 that each of them has two high value areas which are approximately located in the same areas. The two areas with high values are (1) the southwestern mountain front pluvial fans and (2) central western mountain front pluvial fans. After the analysis of landform and the groundwater flow field, it has been found that the areas with high value are the two main groundwater recharge areas. So, it can be determined that there are two main groundwater flow paths in the basin, namely, southwestern mountain front pluvial fans →Touying and mountain front pluvial fans west of Sanying→Heicheng.

The recharge area and recharge elevation have been determined by using the elevation effect of isotopes in the atmospheric precipitation. The average $\delta^{18}O$ elevation gradient in global arid and semi-arid areas (−0.13‰ per 100 m) has been taken as the elevation gradient value of the study area (Clark et al. 1987). In Guyuan, the weighted average value of $\delta^{18}O$ in the precipitation and annual precipitation is −9.11%. The elevations of the two

groundwater recharge areas have been calculated based on the above data.

The recharge area of deep groundwater in the Zhonghe piedmont dip plain is situated at 2,763 m asl. So it can be determined from the regional landform that the long-distance groundwater recharge area of Zhonghe piedmont dip plain is in the Liupanshan Mountains. As for the second groundwater flow zone, the deep groundwater recharge area is at an elevation of 2,485 m asl. The long-distance recharge area of groundwater in the piedmont dip plain in Huangduopu is roughly in the western mountain areas of the basin.

Groundwater renewability analysis

In recent years, the groundwater renewability becomes an important component of groundwater resources assessment, for it is necessary to understand the groundwater circulation and realize the sustainable utilization of groundwater resources. It is essential to ascertain the age of groundwater in the study area for assessing groundwater renewability. In the study, the groundwater age has been obtained by quantitative tritium dating.

Tritium, ^3H, with its half-life ~12.43 years, has been widely used for the estimation of recent groundwater residence time (Fontes 1983; Yurtsever 1983). This is

Fig. 12 Spatial distribution of a ^{18}O concentration and b ^3H concentration
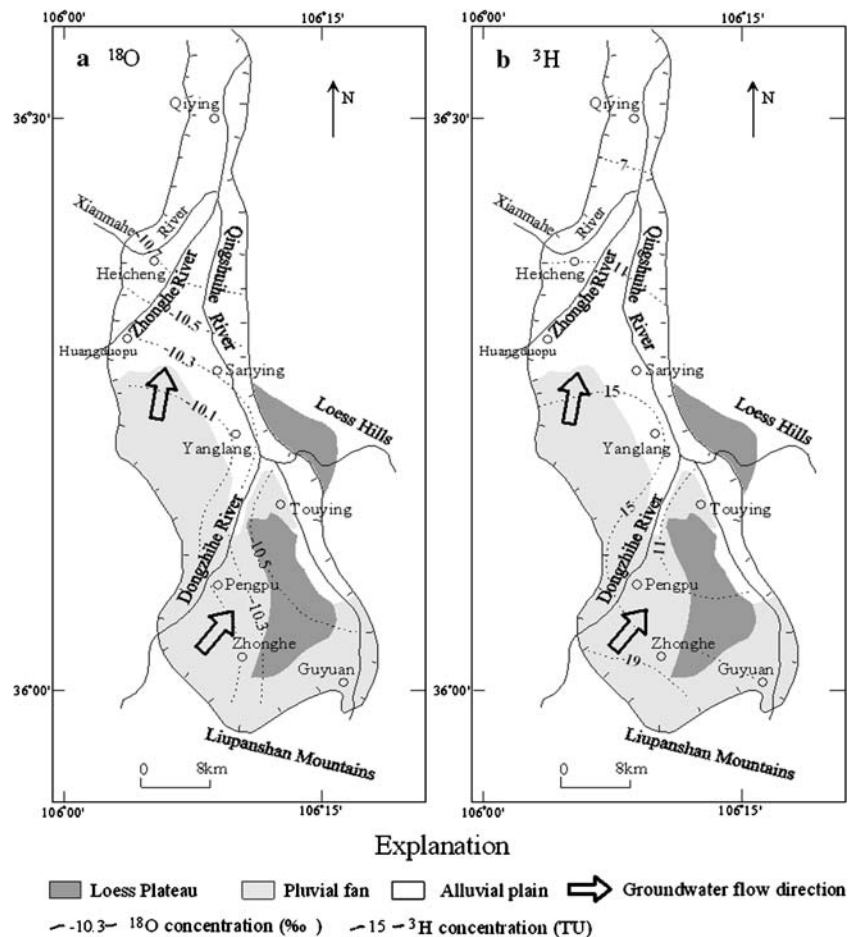
because tritium constitutes part of the water molecule, and thus its behavior is identical to that of any water. Studies have been undertaken to estimate the mean residence time of groundwater in aquifers of different hydrogeological zones using tritium techniques. With the same objective, a mathematical model with exponential distribution function (Fontes 1983; Yurtsever 1983), coupled with the hypothesis of a completely mixed reservoir, was applied to the study area. Practically, this method has proved to be satisfactory for two-dimensional groundwater flow of unlimited planar aquifers (Fontes 1983; Yurtsever 1983). For the SNHAR study area, the required tritium input function for this simulation was taken from the available tritium records at Yinchuan station 230 km away from the study area, which is the closest International Atomic Energy Agency network station to the study area (IAEA 1996). The tritium data obtained for rainfall in Qingshuihe Basin during the period 1996–2001 were also used. The earlier missing tritium data for Yinchuan station during the period 1953–1986 were estimated from the good logarithmic correlation between Yinchuan and Ottawa stations in Canada, which have the longest tritium records globally. The simulated tritium output curves were calculated using the convolution integral expressed:

$$C_0(t) = \sum_{\tau=0}^{\infty} c(t-\tau) \cdot h(\tau) \cdot e^{-\lambda} \qquad (7)$$

where $h(\tau) = \frac{1}{\tau_m} \cdot e^{-(1/\tau_m)t}$ and $\tau_m = \frac{V}{Q}$ where $C_0(t)$ is the concentration at a given time, $C(t-\tau)$ is the input concentration at the time of recharge, t is the time of discharge, τ is the residence time of the water parcel in the aquifer, λ is the radioactive decay constant, τ_m is the mean residence time of the system, and V and Q are, respectively, the volume of groundwater reservoir and the discharge of the system. The calculation of tritium output curves were performed using the program Model, prepared by Yurtsever Y, of the IAEA (Yurtsever 1983). Figure 13 shows the tritium output curves for different values of mean residence time (10, 30, 50, 70, 100, 300, 500 and 1,000 years), together with the tritium input function of Yinchuan station during the period 1950–2001. Groundwater ages can be ascertained from the simulated output curves.

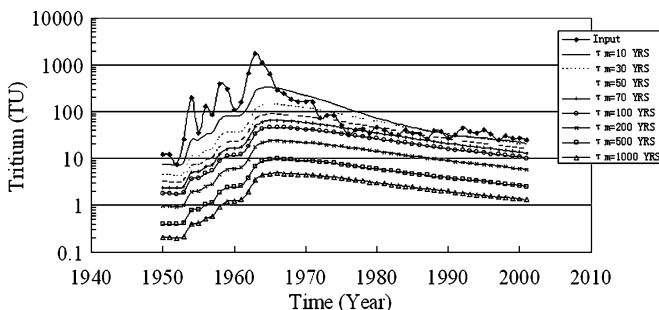Figure 13 suggests that if the average ³H concentration in shallow groundwater of the upper plain (QB01, QB03,

Fig. 13 Calculated tritium output curves for different mean residence times (τ_m) in years

G28, G27) is 21.77 TU, the age is 10 years or so. The average ³H concentration in deep saline groundwater of the lower plain is 4.99 TU, and the age of groundwater is more than 200 years. In the main exploitation areas of the upper plain, the average ³H concentration in deep groundwater (QB02, G29, G51, HX21) is 11.25 TU, and the age of the groundwater ranges between 70 and 100 years. Because of the higher precipitation on the upper plain compared with the lower plain, the faster circulation rates made the deep groundwater accept the modern fresh water more easily in a short time. Groundwater carries a large amount of highly soluble salts to the lower plain, and resulted in high ³H and low TDS in the upper plain. In addition, water quality has been affected by the uncontrolled exploitation of groundwater, which has caused more powerful mixing between the modern shallow groundwater and the deep groundwater.

From the age dating of groundwater, it can be seen that the shallow groundwater in the upper plain circulates quickly and there is strong renewability. The circulation of deep groundwater in the lower plain area is slow with poor renewability. The renewability of deep groundwater in the upper plain is between the two mentioned above. However, in the main groundwater exploitation areas, the speed of water circulation increases and the renewability evidently increases.

Conclusion

Data on hydrogeochemistry and environmental isotopes of water were utilized to understand origin, geochemical evolution, hydraulic interconnection, and renewability of groundwater in Qingshuihe Basin. The main conclusions are as follows: the hydrogeochemical data indicate that fresh groundwater zones of the basin are mainly distributed in the mountain front pluvial fans, and the saline water zones in the lower alluvial plains; the concentration of TDS in groundwater increases along the groundwater flow from south to north; and the most common water types are Na–HCO₃ and Na–SO₄, which dominate the shallow, unconfined groundwater of the mountains front pluvial fans, and the groundwater of the lower alluvial plain, respectively.

Stable isotope data show that there are four types of groundwater which have different origin mechanisms: (1) the shallow groundwater in the mountain front pluvial fans originates from the recent recharge by atmospheric precipitation, (2) the deep paleo-groundwater of the lower alluvial plains was formed a long time ago, (3) the shallow groundwater in the lower alluvial plains has undergone evaporation during the recharging process, and (4) the 'mixed' groundwater is from the mixing of the shallow and deep groundwater in the plain.

Several mechanisms contribute to the subsequent evolution of groundwater chemistry. In the upper pluvial fans, CO_2 gas dissolution, silicates weathering and cation exchange predominate. These reactions can increase concentrations of Na^+ and HCO_3^-. In the lower alluvial

plains, the geochemical evolution of groundwater is related to mineral dissolution. The input of Na^+, SO_4^{2-} and Cl^- is from the dissolution of halite (NaCl) and mirabilite ($Na_2SO_4 \times 10H_2O$) deposited in the Tertiary Formation. The dissolution of gypsum is another possible source of SO_4^{2-}. The evaporative enrichment only produces significant salinity increases in the shallow groundwater of the lower alluvial plains.

Under the present exploitation conditions, there is a mixing relationship of the groundwater in the study area as follows: modern water accounts for 76% in the groundwater of the upper plain, modern water accounts for less than 32% in the groundwater of the lower plain, and modern water accounts for 52~66% in the groundwater of the main exploitation areas (Pengbao exploitation area and Huangduobao exploitation area). The over-exploitation of groundwater intensifies the mixing of shallow groundwater and deep groundwater.

There are two main groundwater flow paths in the basin, namely, southwestern mountain front pluvial fans →Touying, and mountain front pluvial fans west of Sanying→Heicheng. The recharge area of the former flow path is situated in the Liupanshan Mountains, and the latter recharge area is roughly in the western mountain areas of the basin.

The circulation of the shallow groundwater in the upper plain takes 10 years or so, showing a strong renewability. However, the circulation of the deep groundwater in the lower plain area takes more than 200 years, showing a poor renewability. In the main exploitation areas, the renewability of groundwater evidently has increased under the current exploitation conditions, and the circulation period is within the range of 70–100 years.

References

Bigeleisen J, Perlman ML, Prosser HC (1952) Conversion of hydrogenic materials to hydrogen for isotopic analysis. Anal Chem 24:1356–1357

Chen MX, Ma FS (2000) Groundwater resources and the environment in China. Seismological Press, Beijing, pp 132–137

Clark ID, Fritz P, Quinn OP et al (1987) Modern and fossil groundwater in an arid environment: a look at the hydrogeology of Southern Oman. In: Use of stable isotopes in water resources development. IAEA, Vienna, pp 167–187

Epstein S, Mayeda T (1953) Variation of ^{18}O content of water from natural sources. Geochim Cosmochim Acta 4:213–224

Fontes JC (1983) Dating of groundwater. Guidebook on nuclear techniques. Technical Report Series no 91. IAEA, Vienna

Gerla PJ (1992) Pathline and geochemical evolution of groundwater in a regional discharge area, Red River Valley, North Dakota. Ground Water 30:743–754

Hendry MJ, Schwartz FW (1990) The chemical evolution of groundwater in the Milk River Aquifer, Canada. Ground Water 28:253–261

IAEA (International Atomic Energy Agency) (1996) World survey of isotope concentration in precipitation. Environmental isotope data no. 8–10, IAEA, Vienna

Lowry R (1999) Concepts and applications inferential statistics. Vassar College, Poughkeepsie, NY, USA, pp 252–263. http://faculty.vassar.edu/lowry/webtext.html. Cited 25 December 2007

Mahlknecht J, Schneider JF (2004) Groundwater recharge in a sedimentary basin in semi-arid Mexico. J Hydrol 12:511–530

NGMB (Ningxia Geology and Mineral Bureau) (1984) Assessment of groundwater resources in Ningxia province. NGMB Rep 1984, NGMB, Yinchuan, China

NGMB (Ningxia Geology and Mineral Bureau) (1990) Hydrogeological exploration of the domestic water supply in Guyuan and Pengyang county of Ningxia province. Ningxia Geology and Mineral Bureau, NGMB Rep 1990, NGMB, Yinchuan, China

NGMB (Ningxia Geology and Mineral Bureau) (1997) Exploration and development of the fresh groundwater resources in the saline water region of Heicheng. Ningxia Geology and Mineral Bureau, NGMB Rep 1997, NGMB, Yinchuan, China

NGMB (Ningxia Geology and Mineral Bureau) (2000) Five years summary of groundwater monitoring in Guyuan of Ningxia province. Ningxia Geology and Mineral Bureau, NGMB Rep 2000, NGMB, Yinchuan, China

Ningxia Meteorological Bureau of China (1995) Meteorological history of Ningxia province. Meteorological Publishing House, Beijing, pp 21–22

Parkhurst DL (1995) User's Guide to PHREEQC: a computer program for speciation, reaction-path, advective-transport, and inverse geochemical calculation. US Geol Surv Water-Resour Invest No. 95–4227

Payne BR (1988) The status of isotope hydrology today. J Hydrol 100:207–237

Sracek O, Hirata R (2002) Geochemical and stable isotopic evolution of the Guarani Aquifer System in the state of Sao Paulo, Brazil. J Hydrol 10:643–655

US EPA (2003) National primary drinking water regulations. US EPA, Washington, DC

Weaver TR, Bahr JM (1991) Geochemical evolution in the Cambrian-Ordovician Sandstone Aquifer, eastern Wisconsin. 2. Correlation between flow paths and groundwater chemistry. Groundwater 29:510–515

Yurtsever Y (1983) Models for tracer data analysis. In: Guidebook on nuclear techniques in hydrology. Technical Reports, series no 91. IAEA, Vienna

Zhou TX (1984) Tectonism and geomorphology of Ningxia in China. Ningxia People's Publishing House, Yinchuan, China, pp 87–99